Biochemical and Biophysical Research Communications 438 (2013) 295–300

Contents lists available at SciVerse ScienceDirect

Biochemical and Biophysical Research Communications

journal homepage: www.elsevier.com/locate/ybbrc

Validation of Alexa-647-ATP as a powerful tool to study P2X receptor ligand binding and desensitization

Yogesh Bhargava [a,*], Annette Nicke [b], Jürgen Rettinger [a,1]

[a] Department of Biophysical Chemistry, Max-Planck-Institute of Biophysics, Max-von-Laue-Strasse 3, 60438 Frankfurt am Main, Germany
[b] Department of Molecular Biology of Neuronal Signals, Max Planck Institute for Experimental Medicine, 37075 Göttingen, Germany

ARTICLE INFO

Article history:
Received 8 July 2013
Available online 26 July 2013

Keywords:
P2X1 receptor
Allosteric interaction
Binding
Desensitization
Alexa-647-ATP
Ion channel

ABSTRACT

Ion channel opening and desensitization is a fundamental process in neurotransmission. The ATP-gated P2X1 receptor (P2X1R) shows rapid and long-lasting desensitization upon agonist binding. This makes the electrophysiological investigation of its desensitization process, agonist unbinding, and recovery from desensitization a challenging task. Here, we show that the fluorescent agonist Alexa-647-ATP is a potent agonist at the P2X1R and a versatile tool to directly visualize agonist binding and unbinding. We demonstrate that the long-lasting desensitization of the P2X1R is due to both slow unbinding of agonist from the desensitized receptor and agonist mediated receptor internalization. Furthermore, the unbinding of the agonist Alexa-647-ATP from the desensitized receptor is accelerated in the continuous presence of competitive ligand. Modeling of our data indicates that three agonist molecules are required to drive the receptor into desensitization. Direct visualization of ligand unbinding from the desensitized receptor demonstrates the cooperativity of this process.

1. Introduction

The ATP-gated P2X receptors are non-selective cation channels with a high Ca^{2+} permeability. Their physiological roles range from fast excitatory synaptic transmission and neuromodulation to the activation of complex signaling pathways and cytokine release [1,2]. The seven known mammalian P2X receptor subunits assemble into homo- or heterotrimeric ion channels that show varying degrees of desensitization [3]. In particular, the homomeric P2X1 and P2X3 subtypes show a fast and long-lasting desensitization. A single P2X receptor has three intersubunit-ATP binding sites [4,5]. The determination of the crystal structures of the zebrafish P2X4R in the apo- and ATP-bound states [4,6] greatly enhanced our understanding of its molecular structure and revealed details about the mechanism of ATP binding. However, the molecular basis of channel function such as, the number of agonist molecules and the conformational changes required to induce desensitization and the molecular mechanism of the slow recovery from desensitization remain elusive.

In a previous study on oocyte-expressed P2X1R, it was found that 3 nM ATP, a concentration insufficient to show macroscopic receptor activation, induced half maximal receptor desensitization and it was suggested that the high potency of ATP at this receptor is masked by its fast desensitization [7]. This hypothesis was strengthened in a subsequent study using a non-desensitizing P2X2-1 chimera [8]. Similarly, preincubation of the P2X3R with nanomolar ATP concentrations influenced subsequent current responses in patch clamp experiments [9,10]. Two explanations (a) use-dependent inhibition by occupation of a high affinity binding site in the desensitized receptor (Pratt et al.) [10] and (b) occupation of a high affinity binding site in the resting receptor that causes the transition into an intermediate, still closed, receptor state with lower ATP affinity have been suggested. In general, it is assumed that agonist dissociation is the rate-limiting step in recovery from desensitization. In the case of P2X1Rs, internalization and trafficking was also found to influence its recovery from desensitization [11–13]. Besides the long recording times required to determine recovery from desensitization, a difficulty in all functional studies is, that the agonist affinity of the receptor and its occupancy cannot be directly measured. Here we show that the fluorescent ATP-analogue Alexa-647-ATP is a potent P2XR agonist that can be used to directly measure mechanistic details of the P2XR desensitization and resensitization process.

Abbreviations: PAO, phenyl arsine oxide; MgORI, magnesium oocyte Ringer's solution; ORI, oocyte ringer's solution ; VCF, voltage clamp fluorometry.

* Corresponding author. Address: Department of Applied Microbiology, School of Biological Sciences, Dr. Hari Singh Gour Central University, Sagar (M.P.), India.
E-mail address: yogesh.bhargava@gmail.com (Y. Bhargava).
[1] Present address: Multi Channel Systems MCS GmbH, Aspenhaustrasse 21, 72770 Reutlingen, Germany.

0006-291X/$ - see front matter © 2013 Elsevier Inc. All rights reserved.
http://dx.doi.org/10.1016/j.bbrc.2013.07.058

2. Materials and methods

2.1. Materials

ATP (disodium salt), Collagenase, Gentamicin, and phenyl arsine oxide (PAO) were from Sigma–Aldrich Chemie GmbH (Munich, Germany). Alexa-647-ATP as 5 mM concentration in 1X TE buffer was purchased from Molecular Probes, Darmstadt, Germany and stored in small aliquots at −20 °C.

2.2. cRNA synthesis, oocyte injection, and PAO treatment

Capped cRNA of rat His-P2X1R and chimeric His-P2X2-1R [8,14] was synthesized using the SP6 mMESSAGE/mMACHINE kit (Ambion, Austin, TX, USA). *Xenopus laevis* (Nasco International, Fort Atkinson, WI) oocytes were prepared as described [15], injected with 25 ng (wild type rat P2X1) or 5 ng (P2X2-1R chimera) cRNA per cell, and kept in Calcium-Oocyte Ringer (CaORi: 110 mM NaCl, 5 mM KCl, 2 mM $CaCl_2$, 1 mM $MgCl_2$, 5 mM HEPES, pH 7.5) containing 0.05 mg/ml gentamicin. Phenyl Arsine Oxide (PAO) treatment was performed for 1 h with 100 μM PAO in CaORI and oocytes were used within 3–4 h.

2.3. Electrophysiological recordings

Two-electrode voltage-clamp (TEVC) recordings were performed 1–3 days after cRNA injection in MgORi buffer (90 mM NaCl, 1 mM KCl, 2 mM $MgCl_2$, 5 mM HEPES, pH 7.5) as described using a TEC-03X amplifier (NPI electronics, Tamm, Germany), Cell-Works software (NPI electronics), and a fast and reproducible solution exchange [7]. Dose response curves were determined as described [7]. Data are presented as mean ± SEM for the indicated number of experiments (n). EC_{50}, DC_{50}, and BC_{50} values were calculated from a nonlinear fit of the Hill equation using Origin software (OriginLab, Northampton, MA, USA). Graphs were plotted in Origin v7.5 or v8 software.

2.4. Voltage-clamp fluorometry (VCF)

For VCF recordings, a custom-made oocyte chamber was assembled on a Zeiss inverted microscope (Axiovert 35 M) equipped with a FLUOR-20X objective (NA = 0.75) (Zeiss, Germany) as described [16]. The fluorescence was stimulated by a 100 W Tungsten lamp using the XF110-2 filter set (650 nm excitation and 665 nm emission wavelength, Omega Optical, Brattleboro, USA) and was measured through a PIN-022A photodiode (United Detector Technologies, USA) mounted on the eye port of the microscope. Light intensity and duration was regulated by the external amplifier and a TTL controlled shutter (D-122 UniBlitz, Optilas, USA). The signal from the photodiode was amplified by an EPC-5 patch clamp amplifier (HEKA Electronics, Germany) and filtered at 300 Hz. Fluorescence was excited for 1 s every 30 s to prevent bleaching.

Numeric simulations were performed with Gepasi 3.0 software [17].

3. Results and discussion

3.1. Alexa-647-ATP is a potent agonist at the P2X1R

Alexa-647-ATP is a mixed isomer in which the bright far-red fluorescent dye is attached via an aminoethylcarbamoyl linker to the 2′ or 3′ position of the ATP ribose ring. According to VCF studies [18] and the recently published crystal structure of the ATP bound zP2X4R [4] the ribose moiety of the bound ATP is facing the solution and should therefore not greatly interfere with its binding to the receptor. To test the efficacy of Alexa-647-ATP as an agonist, we first compared current responses to identical concentrations of ATP and Alexa 647-ATP. Therefore, the P2X1 receptor was first completely desensitized by application of 30 μM ATP. Then 10 s-pulses of 1 μM ATP and 1 μM Alexa-647-ATP were alternately applied in 1 min intervals. This protocol was used to establish an equilibrium between desensitized and resensitized receptors and to assure that the 1 μM agonist applications were applied to an equal fraction of resensitized receptors, i.e., those that recovered within the 1 min interval (about 5% of the receptors, see also below). As seen in Fig. 1A, Alexa-647-ATP produced about half of the ATP peak response. A full dose–response curve for Alexa-647-ATP at the P2X1R was not determined because of the comparably high agonist concentrations required and the significant costs of Alexa-647-ATP. Instead, we compared the potency of ATP and Alexa-647-ATP at a P2X2-1R chimera in which the intracellular N-terminus and first transmembrane domain of the P2X1R are replaced by the corresponding domains of the P2X2R. This chimera combines the non-desensitizing properties of the P2X2R with nanomolar ATP sensitivity and has been shown to represent a useful model of the P2X1R ligand-binding domain [5,8,15]. At this model, Alexa-647-ATP revealed an about 10-fold lower potency (EC_{50} = 28 ± 7 nM) compared to ATP (EC_{50} = 3 ± 0.1 nM). However, both Alexa-647-ATP and ATP elicited the same maximal current responses in the same oocytes suggesting that Alexa-647-ATP is a full agonist (Fig. 1B and C).

3.2. Optimization of fluorescence recording protocols

After establishing that Alexa-647-ATP binding to P2X1Rs can be specifically detected (see below), we optimized the illumination protocol to prevent photobleaching. Therefore, the time course of fluorescence decrease from P2X1R-expressing oocytes after exposure to 300 nM Alexa-647-ATP were compared under continuous light application and if light was applied in 1 s-pulses in 10 s, 20 s, 30 s, or 40 s intervals. Since no difference in dissociation time-courses was observed between the 30 and 40 s intervals (τ_{30} = 634.8 ± 36.7 s, n = 6; τ_{40} = 633.2 ± 45.1 s, n = 4), 30 s intervals were used in all subsequent experiments. Next, we monitored binding and dissociation rates of Alexa-647-ATP. However, as shown for binding in presence of 100 nM Alexa-647-ATP (Fig. 2A), no steady-state binding was achieved, suggesting that Alexa-647-ATP time-dependently accumulates in an "unspecific" compartment and/or that additional receptors are inserted in the plasma membrane during the measurement. Similarly, no complete washout of fluorescence was achieved even after washing the cells for more than one hour (Fig. 2B). Since P2X1Rs have been reported to be subject of dynamic trafficking and agonist-induced internalization [11–13] we suspected that the residual fluorescence originated from Alexa-647ATP-bound to internalized P2X1Rs. Therefore, we pre-treated the oocytes with PAO which has been shown to inhibit receptor trafficking [19]. This treatment resulted in clear steady-state binding and nearly complete dissociation of bound Alexa-647-ATP (Fig. 2A and B, circles) and was used in all subsequent experiments. Thus, a time constant of 803 ± 7 s was determined for the Alexa-647-ATP dissociation from the completely desensitized P2X1R. This is in good agreement with the functionally determined time constant (696 ± 60 s) for recovery of P2X1Rs from ATP-induced desensitization [7] and demonstrates that all ATP binding sites have to be vacant before the receptor can be activated again. Furthermore, these data suggest that agonist unbinding rather than subsequent conformational change is the rate-limiting step in resensitization. Additionally, a limited receptor population undergoes internalization, as previously proposed.

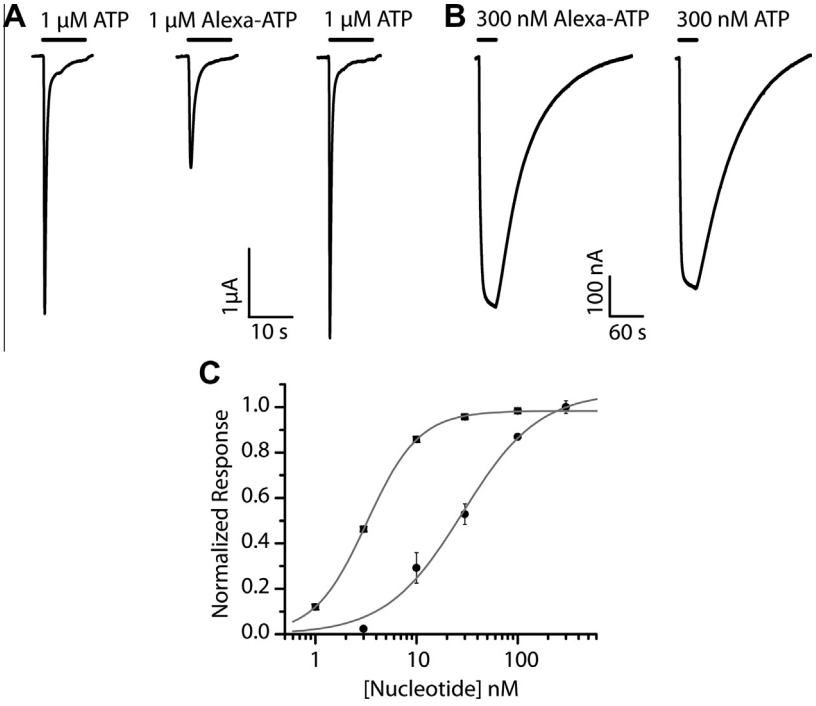

Fig. 1. Agonistic activity of Alexa-647-ATP: (A) Representative P2X1R current traces upon alternating application of 1 μM ATP and 1 μM Alexa-647-ATP. A reproducible equilibrium between desensitized and resensitized receptors was obtained by complete desensitization during each agonist application and 1 min intervals between activations. (B) Representative current traces of the non-desensitizing P2X2-1R chimera after sequential application of 300 nM ATP and Alexa-647-ATP to the same cell. (C) Comparison of the dose response curves of ATP (squares) and Alexa-647-ATP (circles) at the P2X2-1R chimera. Data are presented as mean ± SEM of 5–8 cells.

3.3. Binding kinetics of Alexa-647-ATP at the P2X1R

For ATP, an EC_{50} value of about 1 μM has been determined at oocyte-expressed P2X1Rs. However, already 3 nM ATP, a concentration that does not produce detectable macroscopic currents, are sufficient to induce half maximal desensitization (DC_{50}) [7]. The average number of ATP molecules bound to the P2X1R at this low ATP concentration remained elusive. Therefore, we next used Alexa-647ATP to estimate the number of agonist molecules required to induce desensitization. To this end, we first determined Alexa-647-ATP steady-state binding by applying different test concentrations followed by a 30 nM reference concentration. As expected, application of Alexa-647-ATP to control oocytes resulted in a fast and step-like fluorescence increase that was rapidly reversed after washout of the ligand and corresponded to the free Alexa-647-ATP in solution (Fig. 2C). In contrast, additional slowly increasing and decreasing fluorescence changes were observed on P2X1R-expressing oocytes, indicating specific binding of Alexa-647-ATP to the P2X1Rs (Fig. 2D). Thus, specific and non-specific fluorescence signals could be clearly distinguished due to their different time-courses, and total, specific and unspecific fluorescence changes could be determined individually for each Alexa-647-ATP application (Fig. 2E). A non-linear curve-fit of the Hill equation to these data (Fig. 2F) yielded a half maximal binding value (BC_{50}) of 1.8 ± 0.2 nM (n_H = 0.9 ± 0.1). Note that macroscopic currents cannot be recorded at these low agonist concentrations.

3.4. Concentration dependence of Alexa-647-ATP induced P2X1R desensitization

To correlate the receptor occupancy with the fraction of desensitized receptors at a given Alexa-647-ATP concentration, we next determined the dose-dependent desensitization [7]. Therefore, oocytes were first incubated for 1 h in ligand-free buffer to assure that all receptors are in the resting state. Then, a 10 s-pulse of 30 μM ATP was applied to completely desensitize all receptors and to determine the total peak current (P_E1). After 1 min, a second reference pulse of 30 μM ATP (P_E2) was applied to determine the percentage of receptors that had recovered from desensitization within 1 min (5.1 ± 1.2%, n = 22). To establish the dose-dependent desensitization, oocytes from the same batch were then incubated with the indicated nanomolar concentrations of Alexa-647-ATP and subsequently exposed to two 10 s-pulses of 30 μM ATP at 1 min intervals to obtain the residual peak current ($P_{ER}1$) and the reference current ($P_{ER}2$), respectively. The calculated total peak current (P_C1) was then determined under the assumption that $P_{ER}2$ represents around 5% of P_C1 ($P_C1 = 100 \times P_E2/5$) and the $P_{ER}1$ response was divided by P_C1 to obtain the relative fraction of activatable receptors. Using this protocol, the half maximal desensitization (DC_{50}) was determined at 9 ± 0.5 nM Alexa-647-ATP (n_H = 1.9 ± 0.1, Fig. 3A). The value of receptors recovered from Alexa-ATP-induced desensitization within 1 min (5.1 ± 1.2%) is not significantly different to that previously determined for ATP under the same conditions [7], confirming that both agonists induce very similar long-lasting desensitization.

3.5. Simulation of Alexa-647-ATP concentration dependence of P2X1R desensitization

The Alexa-647-ATP concentration required to desensitize half of the P2X1R population (DC_{50} = 9 nM) is fivefold higher than the concentration for half-maximal binding (BC_{50} = 1.8 nM) suggesting, that at least two of the three ATP binding sites need to be occupied to desensitize the receptor. To determine the number of agonist molecules needed for desensitization, we modeled "desensitization curves" under the assumption that one, two, or three Alexa-647-ATP molecules are required. Therefore, we inserted the experimentally obtained binding data (Fig. 2F) in the following binomial equation to calculate for each Alexa-647-ATP

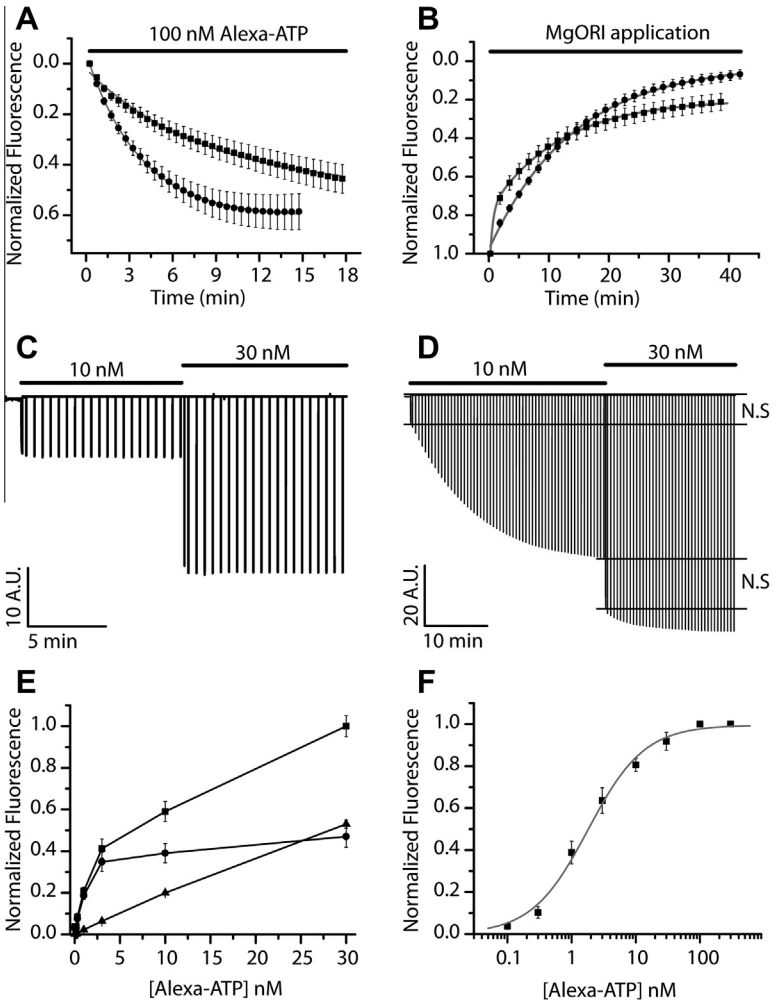

Fig. 2. Specific binding of Alexa-647-ATP to the P2X1R: Representative fluorescence traces from P2X1R-expressing oocytes during (A) association of 100 nM Alexa-647-ATP with (circles) and without (squares) PAO treatment (B) dissociation of 300 nM Alexa-647-ATP with (circles) and without (squares) PAO treatment. For clarity, one in every third data point is plotted. Data are presented as mean ± SEM of 3–6 cells and fitted with mono/bi-exponential fits. Original traces of fluorescence changes after application of different Alexa-647-ATP concentrations to (C) control (non-injected) and (D) P2X1R-expressing cells. The horizontal lines in P2X1R-expressing cells separates specific from non-specific (N.S.) signals. The vertical dark lines indicate individual 1 s fluorescence measurements interrupted by 30 s shutter closures to prevent bleaching. Note that no currents could be recorded at these low ATP concentrations and parallel current traces are therefore not shown. (E) Specific P2X1R bound Alexa-647-ATP fluorescence (circles), non-specific fluorescence (triangles), and total Alexa-647-ATP fluorescence (squares) measured after steady-state binding. Data are presented as mean ± SEM of 3–9 cells. (F) Alexa-647-ATP binding curve at the P2X1R determined under steady-state condition. Data represent mean ± SEM of 3–9 cells.

concentration the statistical distribution of P2X1Rs occupied by none, one, two, or three molecules (Table 1):

$$f(x) = \frac{n!(p^x q^{n-x})}{[(n-x)!x!]} \quad (1)$$

In this equation, n is the total number of ligand binding sites per receptor ($n = 3$), p is the probability that Alexa-647-ATP is bound (Fig. 2F and Table 1); q is the probability that a binding site is not occupied ($1-p$), and x is the number of bound Alexa-647-ATP molecules per receptor. Functional responses were then calculated for following three different assumptions:

(1) *One-site*: If binding of one agonist molecule per receptor is sufficient for desensitization, ATP would produce functional response only from the non-desensitized $f(0)$ population.
(2) *Two-site*: If binding of at least two agonist molecules is required, ATP would produce functional response only from the non-desensitized $f(0) + f(1)$ population.
(3) *Three-site*: If binding of three agonist molecules is required, ATP would produce functional response only from the non-desensitized $f(0) + f(1) + f(2)$ population.

Fitting of the Hill equation to the calculated values (Table 1) revealed half maximal desensitization for Alexa-647-ATP at 0.6 ± 0.01 nM, 1.6 ± 0.1 nM, and 8.6 ± 0.09 nM (n_H of 1.9 ± 0.05, 1.3 ± 0.01 and 1.1 ± 0.1 respectively) for the one- two-, and three-site assumption, respectively (Fig. 3B). The high degree of overlap between the curve derived from the "three-site" assumption (Fig. 3B, circles) and the experimentally determined data (Fig. 3B, dotted line) strongly indicate that binding of three Alexa-647-ATP molecules is required for P2X1R desensitization. This finding is in agreement with Bhargava et al. [15], but might on the first sight disagree with a recent study in which it was shown that two ATP molecules are sufficient for P2X2 channel opening [20]. However, the P2X2R does not show fast desensitization and likely has a different activation mechanism. It has to be noted, however, that cooperative binding [21,22], was neglected in our model for simplicity.

3.6. Agonist dissociation from the desensitized receptor is a cooperative process

300 nM Alexa-647-ATP is sufficient to completely desensitize P2X1Rs and a dissociation rate of 803 ± 7 s was measured upon re-

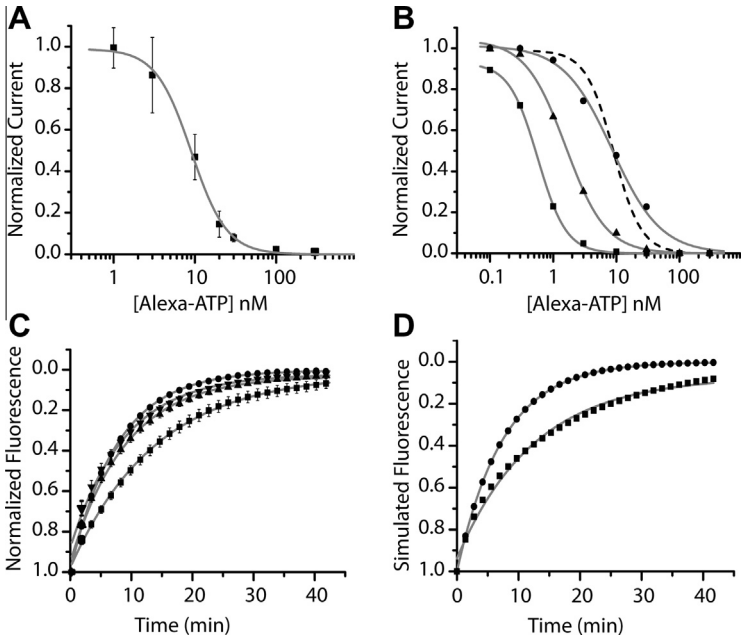

Fig. 3. Analysis of the P2X1R desensitization and resensitization process: (A) Desensitization of the P2X1R induced by different Alexa-647-ATP concentrations. Data are presented as mean ± SEM of 5–33 cells. (B) Simulation of P2X1R desensitization under the assumption that one (squares), two (triangles) or three (circles) Alexa-647-ATP molecules are required to induce desensitization (Table 1). For comparison, the experimentally determined desensitization curve (as in A) is shown as a dotted line. (C) Time course of Alexa-647-ATP fluorescence decay from the P2X1R measured in the presence of MgORI (squares), ATP (10 μM) (inverted triangles), TNP-ATP (300 nM) (circles) and NF449 (100 nM) (triangles). For clarity, one in every third data point is plotted. Data are represented as mean ± SEM of 3–7 cells. All traces were fitted with mono-exponential functions and normalized to the level of fluorescence obtained after 15 s from the onset of Alexa-647-ATP dissociation in each measurement. (D) Simulation of the Alexa-647-ATP dissociation kinetics in the presence (circles) and absence (squares) of competing ligands.

Table 1
Experimentally determined desensitized P2X1Rs and simulated populations of P2X1Rs bound to 0, 1, 2 and 3 Alexa-647-ATP molecules at different Alexa-647-ATP concentrations.

Alexa-647-ATP (nM)	P^1	$f(0)$	$f(1)$	$f(2)$	$f(3)$
0.1	0.04 ± 0.01	0.89	0.1	0.004	0
0.3	0.1 ± 0.03	0.72	0.25	0.03	0.001
1	0.39 ± 0.05	0.23	0.44	0.28	0.0
3	0.64 ± 0.06	0.048	0.25	0.44	0.26
10	0.81 ± 0.03	0.007	0.09	0.38	0.52
30	0.92 ± 0.04	5.5E−4	0.02	0.21	0.77
100	1	0	0	3E−4	0.99
300	1	0	0	3E−4	0.99

P^1 denotes probability that a receptor is labeled; $f(0)$, $f(1)$, $f(2)$ and $f(3)$ denotes fractional population of receptors with 0, 1, 2 and 3 Alexa-647-ATP bound receptors respectively.

moval. The use of Alexa-647-ATP as a fluorescent agonist enables to test whether dissociation rate differs in presence of other ligands of P2X1Rs. To this end, Alexa-647-ATP dissociation was determined in the presence of high concentrations of ATP (10 μM, DC_{50} = 3 nM) or the competitive antagonists TNP-ATP (300 nM, IC_{50} = 1 nM) or NF449 (100 nM, IC_{50} = 0.3 nM). Presence of these competitive ligands at these super-saturating concentrations guarantees that all three binding sites are always occupied. Interestingly, accelerated dissociation rates with time constants of 579 ± 3 s (ATP), 474 ± 8 s (TNP-ATP) and 587 ± 32 s (NF449) in contrast to 803 ± 7 s (in the absence of competing ligands) (Fig. 3C), were observed. We hypothesized that ATP-affinity increases after dissociation of the first molecule (i.e., remaining bound agonist molecules would dissociate with slower kinetics) if the empty binding site is not immediately reoccupied by another ligand. We tested this hypothesis by simulating both conditions (rate of dissociation of bound Alexa-647-ATP in presence and absence of saturating competing ligands) using Gepasi software (Fig. 3D). Using a kinetic model with 3 binding sites and two different dissociation rates with k_{off}-fast = 1.72×10^{-3} s^{-1} for dissociation of the first Alexa-647-ATP molecule (for the complete occupancy state) and k_{off}-slow = 0.96×10^{-3} s^{-1} for the dissociation of the second and last Alexa-647-ATP led to time courses with time constants of 580 and 803 s in presence and absence of ligand, respectively, identical to the experimentally determined values, thus, supporting our above hypothesis.

In conclusion, identification of the agonistic activity of Alexa-647-ATP provides an important tool for the real time and parallel measurement of functional state and agonist binding and helped to decipher molecular details of P2X1R desensitization and resensitization.

Acknowledgments

This work was supported by a grant from the DFG (RE2711/1-1) to JR and AN. YB was financed by the International Max Planck Research School (IMPReS). The authors thank Prof. Ernst Bamberg for generous support.

References

[1] K. Kaczmarek-Hajek, E. Lorinczi, R. Hausmann, A. Nicke, Molecular and functional properties of P2X receptors – recent progress and persisting challenges, Purinergic Signal. 8 (2012) 375–417.
[2] B.S. Khakh, R.A. North, Neuromodulation by extracellular ATP and P2X receptors in the CNS, Neuron 76 (2012) 51–69.
[3] C. Coddou, Z. Yan, T. Obsil, J.P. Huidobro-Toro, S.S. Stojilkovic, Activation and regulation of purinergic P2X receptor channels, Pharmacol. Rev. 63 (2011) 641–683.
[4] M. Hattori, E. Gouaux, Molecular mechanism of ATP binding and ion channel activation in P2X receptors, Nature 485 (2012) 207–212.
[5] B. Marquez-Klaka, J. Rettinger, Y. Bhargava, T. Eisele, A. Nicke, Identification of an intersubunit cross-link between substituted cysteine residues located in the putative ATP binding site of the P2X1 receptor, J. Neurosci. 27 (2007) 1456–1466.

[6] T. Kawate, J.C. Michel, W.T. Birdsong, E. Gouaux, Crystal structure of the ATP-gated P2X(4) ion channel in the closed state, Nature 460 (2009) 592–598.
[7] J. Rettinger, G. Schmalzing, Activation and desensitization of the recombinant P2X1 receptor at nanomolar ATP concentrations, J. Gen. Physiol. 121 (2003) 451–461.
[8] J. Rettinger, G. Schmalzing, Desensitization masks nanomolar potency of ATP for the P2X1 receptor, J. Biol. Chem. 279 (2004) 6426–6433.
[9] A. Grote, M. Hans, Z. Boldogkoi, A. Zimmer, C. Steinhauser, R. Jabs, Nanomolar ambient ATP decelerates P2X3 receptor kinetics, Neuropharmacology 55 (2008) 1212–1218.
[10] E.B. Pratt, T.S. Brink, P. Bergson, M.M. Voigt, S.P. Cook, Use-dependent inhibition of P2X3 receptors by nanomolar agonist, J. Neurosci. 25 (2005) 7359–7365.
[11] J.L. Dutton, P. Poronnik, G.H. Li, C.A. Holding, R.A. Worthington, R.J. Vandenberg, D.I. Cook, J.A. Barden, M.R. Bennett, P2X(1) receptor membrane redistribution and down-regulation visualized by using receptor-coupled green fluorescent protein chimeras, Neuropharmacology 39 (2000) 2054–2066.
[12] S.J. Ennion, R.J. Evans, Agonist-stimulated internalisation of the ligand-gated ion channel P2X(1) in rat vas deferens, FEBS Lett. 489 (2001) 154–158.
[13] U. Lalo, R.C. Allsopp, M.P. Mahaut-Smith, R.J. Evans, P2X1 receptor mobility and trafficking; regulation by receptor insertion and activation, J. Neurochem. 113 (2010) 1177–1187.
[14] A. Nicke, H.G. Baumert, J. Rettinger, A. Eichele, G. Lambrecht, E. Mutschler, G. Schmalzing, P2X1 and P2X3 receptors form stable trimers: a novel structural motif of ligand-gated ion channels, EMBO J. 17 (1998) 3016–3028.
[15] Y. Bhargava, J. Rettinger, A. Mourot, Allosteric nature of P2X receptor activation probed by photoaffinity labelling, Br. J. Pharmacol. 167 (2012) 1301–1310.
[16] A. Mourot, E. Bamberg, J. Rettinger, Agonist- and competitive antagonist-induced movement of loop 5 on the alpha subunit of the neuronal alpha4beta4 nicotinic acetylcholine receptor, J. Neurochem. 105 (2008) 413–424.
[17] P. Mendes, Biochemistry by numbers: simulation of biochemical pathways with Gepasi 3, Trends Biochem. Sci. 22 (1997) 361–363.
[18] E. Lorinczi, Y. Bhargava, S.F. Marino, A. Taly, K. Kaczmarek-Hajek, A. Barrantes-Freer, S. Dutertre, T. Grutter, J. Rettinger, A. Nicke, Involvement of the cysteine-rich head domain in activation and desensitization of the P2X1 receptor, Proc. Natl. Acad. Sci. USA 109 (2012) 11396–11401.
[19] F. Vacca, M. Giustizieri, M.T. Ciotti, N.B. Mercuri, C. Volonte, Rapid constitutive and ligand-activated endocytic trafficking of P2X receptor, J. Neurochem. 109 (2009) 1031–1041.
[20] O. Stelmashenko, U. Lalo, Y. Yang, L. Bragg, R.A. North, V. Compan, Activation of trimeric P2X2 receptors by fewer than three ATP molecules, Mol. Pharmacol. 82 (2012) 760–766.
[21] S. Ding, F. Sachs, Single channel properties of P2X2 purinoceptors, J. Gen. Physiol. 113 (1999) 695–720.
[22] A.D. Michel, L.J. Chambers, W.C. Clay, J.P. Condreay, D.S. Walter, I.P. Chessell, Direct labelling of the human P2X7 receptor and identification of positive and negative cooperativity of binding, Br. J. Pharmacol. 151 (2007) 103–114.